Research Article

Journal of Physical Organic Chemistry

Received: 7 April 2008, Revised: 20 June 2008, Accepted: 20 June 2008, Published online in Wiley InterScience: 21 July 2008

(www.interscience.wiley.com) DOI 10.1002/poc.1425

Chlorination of ammonia and aliphatic amines by Cl_2: DFT study of medium and substituent effects

Valerije Vrček[a]* and Hrvoje Meštrić[b]

The mechanism of chlorination of ammonia and aliphatic amines by Cl_2 was studied by quantum-chemical calculations using a series of DFT functionals. Three different reaction pathways were considered for the reaction between Cl_2 and NH_3 in the gas phase. Several intermediates and transition state structures, not described earlier, were located on the corresponding potential energy surface. It is calculated that the reaction field effects (SCIPCM) on the chlorination is much less pronounced than the effect of a specific solvent interaction which was modeled by an explicit water molecule. It is also found that the calculated energy barrier and the reaction free energy of the chlorination of different amines are dependent on the alkyl-substituent effects. With increase in the basicity of amine, the chlorination reaction becomes more feasible. Calculated geometries of intermediates and overall reaction energetics are significantly influenced by the method for a treatment of electron correlation (DFT *vs.* MP2), and by the fraction of HF exchange (χ) in DFT functionals. With increase in the χ in the corresponding functional, the DFT results approach those obtained at the MP2 level, and are closer to experimental values, as well. Copyright © 2008 John Wiley & Sons, Ltd.

Supporting information may be found in the online version of this article.

Keywords: quantum chemical calculation; chlorination; aliphatic amines; reaction mechanism; solvent effect; substituent effect

INTRODUCTION

Chlorination reactions play an important role in environmental chemistry and biochemistry. Water chlorination is the most widely used method for water disinfection, whereas free chlorine is also used extensively in the treatment of wastewaters and in food industry as the principal sanitizing agent. The drawback of chlorination is the formation of a wide range of chlorinated by-products, some with carcinogenic and/or mutagenic properties.[1–5] In addition to this environmental impact, the chlorination reactions are also relevant to physiological processes. Thus, the chlorinating agents, hypochlorous acid (HOCl) and chlorine (Cl_2), are reactive oxidants generated by phagocytes, which are important in host defenses, inflammation, or diabetes and neurodegenerative processes resulted from chlorinative stress.[6–8] The microbicidal and toxic properties of HOCl and Cl_2 stem from their chemical reactivities which include chlorination of amines, unsaturated lipids, and many other biological compounds.[9,10]

The chlorinating intermediate in typical halogenation reactions is generally believed to be HOCl or its conjugate base hypochlorite (ClO^-). HOCl is a ubiquitous chlorinating agent and it is known that chlorination by HOCl involves assistance of water molecules. Both experimental[11,12] and theoretical[13] studies postulated the presence of water in the transition state for the aqueous chlorination of amines by HOCl. However, in organic solvent or in hydrophobic environment, such as in the active site of the enzyme, where no water molecule is present, different mechanisms of chlorination are to be considered. It is shown, for example, that the L-tyrosine in aprotic non-polar solvent, such as hexane, could be easily chlorinated,[14] in a reaction obviously not catalyzed by water.

HOCl is in equilibrium with molecular chlorine (Cl_2), raising possibility that Cl_2 executes halogenation reactions that have previously been attributed to $HOCl/ClO^-$. For example, the reactive intermediate in cholesterol chlorination performed by myeloperoxidase is Cl_2, and not HOCl itself, as suggested earlier.[15] As well, experimental results on chlorination of the cytosine in bacterial RNA suggest that an actual chlorinating agent in this reaction is molecular chlorine derived from HOCl.[16]

At low pH (e.g., in gastric fluid) Cl_2 should be considered again as an important chlorinating agent, even more efficient than HOCl. Indeed, Cl_2 was found to be a much more effective chlorinating agent than either HOCl or NH_2Cl.[17–20]

Finally, the evidence that Cl_2 alone, without water participation, should be considered as an effective chlorinating agent comes from gas-phase studies which shows that ammonia reacts

* *Correspondence to: V. Vrček, Faculty of Pharmacy and Biochemistry, University of Zagreb, A. Kovačića 1, 10000 Zagreb, Croatia.*
E-mail: valerije@pharma.hr

a *V. Vrček*
Faculty of Pharmacy and Biochemistry, University of Zagreb, A. Kovačića 1, 10000 Zagreb, Croatia

b *H. Meštrić*
Faculty of Natural Sciences, Mathematics and Kinesiology, University of Split, N. Tesle 12, 21000 Split, Croatia

with Cl_2 to form either chloroamine or nitrogen trichloride.[21] This gas-phase reaction is not only relevant to both chlorine inhalation studies[22–23] but also to the food industry where chlorine gas is used as an oxidizing and bleaching agent.[24]

Our goal is, by studying reaction mechanism using modern quantum-chemical methods, to compare the chlorination capacity of two closely related species HOCl and Cl_2. Comparative study on chlorination mechanisms involving either HOCl and Cl_2 is warranted due to the results demonstrating that these two oxidants become reactive chlorinating species under different reaction conditions; they react with different rates,[18] and with different biological targets.[14,15]

The preliminary density functional study on the chlorination of ammonia by HOCl is already published,[13] therefore we set out to study an analogous reaction between Cl_2 and amines. In this paper we present that the detailed mechanism of this elementary yet so intricate reaction can be successfully described using modern quantum-chemical DFT methods. Several new intermediates, not described earlier, were located and new reaction pathways were considered. As well, the dependence of the N-chlorination reaction on both solvent and substituent effect was calculated. It is our hope that these results may be useful in future experimental studies of the chlorination reaction at nitrogen, particularly in the gas phase or in organic solvents.

COMPUTATIONAL METHODS

The quantum-chemical calculations were performed using the Gaussian03 suite of programs.[25] All structures were fully optimized (in specified symmetry) using density functional theory (DFT) methods employing several different functionals. Thus, two local functionals, G96LYP[26,27] and TPSS,[28] and four nonlocal functionals, B3LYP,[29–32] B1B95,[33,34] MPWB1K,[33,35,36] and M05-2X,[37] were tested. G96LYP is the generalized gradient approximation (GG method) that depends on both the local spin density and its gradient, whereas TPSS is meta GGA that also depends on local spin kinetic energy. B3LYP is the most popular hybrid method, whereas B1B95 ($\chi = 25$), MPWB1K ($\chi = 44$), and M05-2X ($\chi = 56$) are hybrid meta functionals with successively increased fraction of HF exchange (χ) in the corresponding functional. The 6–31 + G(d,p) basis set (which adds diffuse and polarization functions to heavy atoms and polarization functions to the hydrogens as well) was used for geometry optimizations and frequency calculations. It was reported earlier that this double zeta quality basis set is usually reasonable for comparative purposes.[38] For comparison, all structures were optimized at the MP2/6–31 + G(d,p) level,[39,40] as well. We have found that geometries and relative energies of several intermediates are significantly influenced by using either second-order Møller–Plesset perturbation theory or different fraction of HF exchange (χ) in the corresponding functionals. The effect of different basis set was also tested (see Supplementary Information), but the relative energy order was not perturbed.

Optimized coordinates of all structures are included in the Supplementary Information. Analytical vibrational analysis at the corresponding level was performed to characterize each stationary point as a minimum (NImag = 0) or first-order saddle point (NImag = 1). IRC calculations (intrinsic reaction coordinate as implemented in Gaussian 03) were performed at the corresponding level of theory to identify the minima connected through the transition state. The initial geometries used were that of the corresponding transition states structures, and the paths were followed in both directions from that point. This method verified that a given transition structure indeed connected the presumed energy minimum structures.[41]

Geometry optimization and frequency calculations in the presence of solvent were carried out for all structures at the B3LYP/6–31 + G(d,p) and M05-2X/6–31 + G(d,p) levels. The solvent effects were calculated using the self-consistent reaction field (SCRF) method based on the self-consistent isodensity polarizable continuum method (SCI-PCM),[42] which employs a higher order cavity whose volume and shape are iteratively computed from the electron density. This method has been proposed as a general-purpose way of calculation of the solvent effect on chemical equilibria and reactions.[43–46] The default value of 0.0004 was used for the isodensity surface, 974 points were used in the special grid option, and surface integrals were evaluated using the single center procedure.[47] The solvent relative permittivity of $\varepsilon = 46.7$ (dimethylsulfoxide, DMSO) was used. Numerical frequencies at the corresponding level were calculated for each structure, confirming that structures were minima or first-order saddle points.

The counterpoise correction (CP)[48] for the basis set superposition error (BSSE) has been used in both geometry optimizations and frequency calculations for selected structures.

RESULTS AND DISCUSSION

Chlorination of ammonia by free chlorine molecule corresponds to a type II S_N2 reaction, analogous to, for example, the Menshutkin reaction,[49] where a system consists of a neutral nucleophile and substrate. As is typical of S_N2 reactions in the gas phase, separated reactants NH_3 and Cl_2 initially collapse to an intermediate which is either a van der Waals reactant complex or a "charge-transfer" complex (**1a** in Fig. 1). Isolation and characterization of the transient complex $H_3N\cdots Cl_2$ in the gas phase have been performed earlier.[50,51] It is shown that the reaction between NH_3(g) and Cl_2(g) results in the formation of a weak complex in which the molecular interaction is mainly electrostatic in origin and charge-transfer effects are small. As well, several computational studies of this $H_3N\cdots Cl_2$ complex have been performed analyzing the nature of molecular interaction,[52–55] but none used the DFT method to describe this system.

This molecule-pair reactant has a linear geometry with C_{3v} symmetry, and is calculated lower in energy than the separated reactants (NH_3 and Cl_2) if local functionals (G96LYP or TPSS) were used for calculations (Table 1). However, when hybrid (nonlocal) functionals (such as B3LYP, B1B95, MPWB1K, or M05-2X) are employed, the reaction $NH_3 + Cl_2 \rightarrow$ **1a** becomes endergonic (by 1.7–2.7 kcal mol^{-1}). It is known that the absence of the Hartree–Fock exchange in the generalized gradient approximation (GG) tends to overestimate the strength of this intermolecular interaction,[56] which is also reflected in the shorter N—Cl intermolecular distances obtained with the GGA methods (G96LYP or TPSS). All hybrid functionals provide larger N—Cl intermolecular distances (see Supplementary Information) which are closer to the MP2 calculated distance and to the available experimental value.[57] As expected, the Cl—Cl stretching frequency is the normal mode that suffers the greatest change with the interaction in the complex **1a**. The M05-2X functional yields value of 462 cm^{-1} which is in excellent

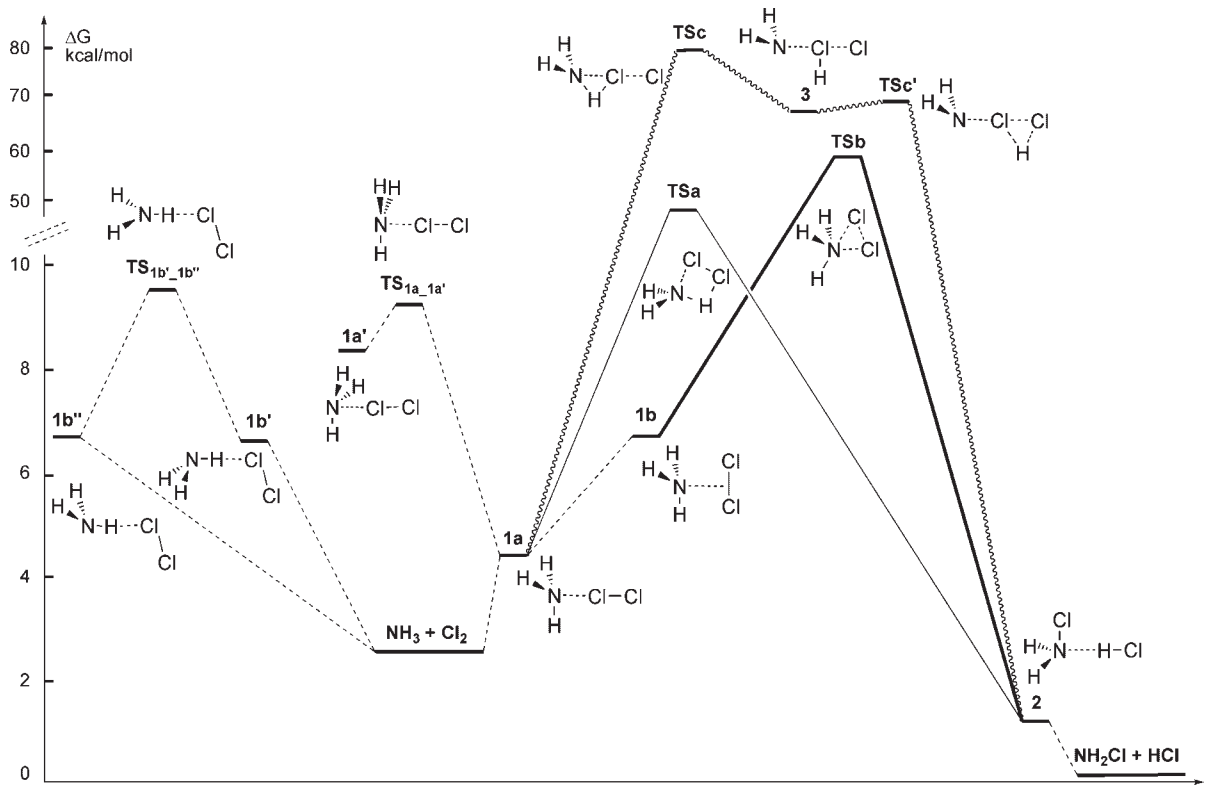

Figure 1. Schematic M05-2X/6–31 + G(d,p) potential energy profile for $NH_3 + Cl_2$ reaction (pathway A, solid line; pathway B, bold line; pathway C, wavy line)

Table 1. Relative[a] free energy (ΔG)[b] differences (in kcal mol^{-1}) for intermediates, transition state structures involved in pathways A, B, and C, calculated at the different levels of theory[c]

Structure	G96LYP χ[d] = 0	TPSS χ = 0	B3LYP χ = 25	B1B95 χ = 25	MPWB1K χ = 44	M05-2X χ = 56	MP2
$NH_3 + Cl_2$	1.6	3.0	2.1	3.4	3.5	2.6	5.0
1a	1.5	0.9	2.5	5.2	6.2	4.3	7.3
1a′	—	—	7.8	9.5	10.1	8.2	6.3
$TS_{1a\_a'}$	—	—	8.1	10.8	10.8	9.0	12.6
1b′	—	5.9	4.8	—	—	6.3	9.0
1b″	—	6.8	4.8	—	—	6.3	7.7
1b	—	—	—	9.1	8.5	6.8	8.3
$TS_{1b'\_b''}$	—	6.5	5.0		—	9.6	11.5
3	55.8	55.0	62.3	—	—	68.3	72.9
TSa	41.2	42.7	49.0	—	—	—	—
TSb	42.6	43.0	49.3	56.4	62.8	59.9	63.6
TSc	58.8	59.0	69.1	74.6	81.2	79.4	73.1
TSc′	55.6	54.8	62.4	—	—	68.1	73.6
4	48.8	50.8	59.7	67.6	76.8	73.7	—
5	60.0	60.6	9.3	76.1	83.0	82.9	95.9
6	59.4	59.3	69.0	75.9	83.6	81.9	88.4
2	3.6	1.1	1.8	3.0	1.9	1.3	1.2
2′	13.1	11.7	17.0	19.7	—	—	—
$TS_{2\_2'}$	13.4	12.0	17.6	20.8	—	—	—
$NH_2Cl + HCl$	0	0	0	0	0	0	0

[a] Relative energies with respect to separated products NH_2Cl and HCl.
[b] At 298.15 K.
[c] Basis set 6–31 + G(d,p) used throughout.
[d] χ, percentage of HF exchange in the functional.

agreement with the experimental frequency (460 cm^{-1}).[58] This indicates that the inclusion of HF exchange is an important parameter for the accurate description of this complex (see Supplementary Information).

An additional complex **1a′** also with linear geometry and C_{3v} symmetry was located, but is calculated less (by 3.9–5.3 kcal mol^{-1}) stable than the complex **1a**. This structure **1a′** has not been described earlier, neither experimentally[50,51] nor theoretically.[52–55] At all hybrid DFT levels it is a real minimum which is easily converted via the transition state structure $\mathbf{TS_{1a\_1a'}}$ back to **1a** (Fig. 1). The calculated energy barrier for this process **1a′** → **1a** is between 0.3 kcal mol^{-1} (B3LYP) and 1.3 kcal mol^{-1} (B1B95) indicating a flat region at the corresponding energy hypersurface. The imaginary frequency (353*i*–568*i* cm^{-1}) corresponds to the nitrogen passing through the plane of the three hydrogens (the ammonia molecule can turn itself inside-out via the so-called umbrella mode).[59–63]

In addition to complexes **1a** and **1a′**, in which chlorine interacts with ammonia in a linear fashion, three more complexes were located as true minima, of which the two are stabilized by weak intermolecular hydrogen bonds (**1b′** and **1b″**), and one is characterized by the T-shaped interaction between nitrogen atom and chlorine molecule (**1b**). The hydrogen-bonded complexes were calculated less stable than **1a** (at all levels employed). They exist in fast, almost degenerate, equilibrium (Fig. 1). The transition state structure $\mathbf{TS_{1b'\_b''}}$ for this interchanging reaction is analogous to $\mathbf{TS_{1a\_a'}}$ which connects complexes **1a** and **1a′**. The only imaginary frequency corresponds to the nitrogen passing through the plane of the three hydrogens (see above). The similar hydrogen-bonded complexes between ammonia and ClF were described recently.[64] However, the existence of complexes **1b′** and **1b″** is somewhat controversial, as different functionals used for calculations resulted in different conclusion about the nature of the corresponding stationary points. For comparison, at the MP2 level of theory the structures **1b′** and **1b″** were located as real minima, which is in agreement with results obtained at the M05-2X level, the exchange-correlation functional shown to be superior for an accurate description of noncovalent interactions.[37]

The structure **1b** is a real minimum when any of the hybrid meta-GGAs methods were employed, being 2.5 kcal mol^{-1} less stable than **1a** at the M05-2X level (only 1 kcal mol^{-1} at the MP2 level). In conclusion, all the five different interaction complexes between ammonia and chlorine, labeled through **1a**–**1b″**, can be located only at the M05-2X and MP2 level of theory. These results show that both the charge transfer and hydrogen-bonded complexes are difficult task for density functionals which should be used systematically and with caution.[65,66]

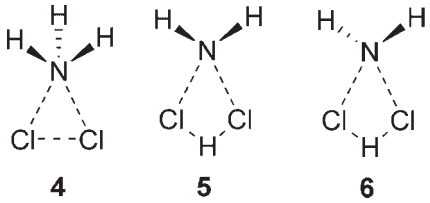

Scheme 1.

All starting complexes with a N—Cl—Cl bond angle different from 180° converged back to **1a** during optimization procedures. These are supposedly symmetrical structures (C_s point group) that would result from an angular oscillation of the Cl_2 subunit as proposed by Legon[50,51] while discussing internal dynamics of the linear complex $H_3N\cdots Cl—Cl$. Only symmetrical structures **4** (∠(N—Cl—Cl) = 45.5°)), **5**, and **6** could be located (Scheme 1), but all were characterized as transition state structures (NImag = 1). The three-membered ring structure **4** is a very unstable complex (Table 1), and is similar in geometry to the front-side attack transition states $(CF_3Cl_2)^-$ and $(CH_3Cl_2)^-$ reported earlier.[67,68] The four-membered ring structures **5** and **6**, in which a hydrogen is positioned between the two chlorine atoms, are even less stable than **4**. While in the case of ammonia the formation of these structures is energetically very unfavorable, it is possible that such high-energy intermediates may be more important in chlorination of some other amines.

As suggested by Bürger,[69] a molecular complex $H_3N\cdots Cl_2$ should be classified as a prereactive complex in which separation of the ammonia and chlorine (in our case the calculated N—Cl interaction distance in **1a** is *ca.* 2.5 Å, whereas the distance between the N atom and the Cl—Cl bond-midpoint in **1b** is *ca.* 2 Å; at the M05-2X level) is notably shorter than the van der Waals contact (N—Cl distance of *ca.* 3.4 Å), but longer than an electron pair bond or an ionic bond. In contrast to van der Waals complexes, which fall apart reversibly into their constituents, the prereactive complex may undergo a reaction to form different products. Indeed, we have found that a chlorine transfer to the unprotonated nitrogen, formally as Cl^+, could proceed via transition state structures **TSa** or **TSb** (Fig. 2, B3LYP results), suggesting that at least two different reaction pathways A and B could be followed along the total reaction coordinate (Fig. 1). However, when meta hybrid functionals (or MP2 method) were employed for calculations the transition state structure **TSa** has vanished from the corresponding energy surface. This structure is not a relevant structure in the chlorination mechanism of ammonia in the gas phase until solvent effects are included (see below). The transition structure **TSb** has a "staggered" confor-

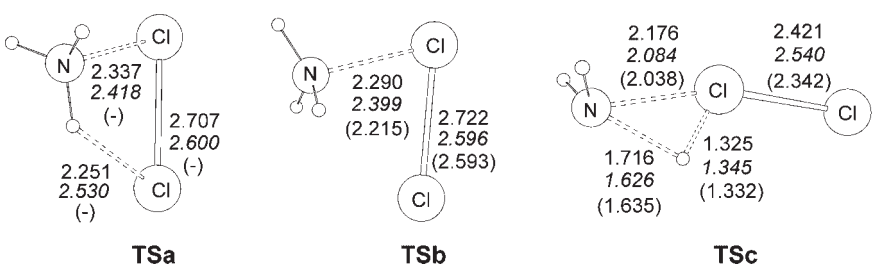

Figure 2. B3LYP/6–31 + G(d,p) optimized geometries of transition state structures TSa, TSb, and TSc for the gas-phase chlorination of NH_3. Bond distances are in angstroms (SCIPCM-B3LYP values in italics and M05-2X values in parentheses)

mation and is characterized by one imaginary frequency ($455i\,cm^{-1}$) which corresponds to the Cl—Cl bond cleavage process simultaneous with N—Cl bond formation. The cyclic structures of **TSb** differ from that of the Menshutkin type of reaction (e.g., Cl^+ transfer in $CH_3Cl\cdots NH_3$ complex) in which the corresponding transition state structure retains C_{3v} symmetry and linear arrangement of the nucleophile and substrate.

The IRC calculation with meta hybrid GGAs shows that transition structure **TSb** connects **1b** and **2**. These results suggest that the linear complex **1a** has to be converted to the T-shaped interaction complex **1b** in order to undergo the chlorine transfer reaction via the transition structure **TSb**.

The structure **2** is a hydrogen-bonded complex (at the M05-2X level the calculated distance $ClH\cdots NH_2Cl$ is 1.821 Å, and the corresponding bond angle Cl—H—N is 176.1°) in which the separation of the two constituents leads without a barrier to the final products, the chloroamine (NH_2Cl) and hydrochloric acid (HCl). This product interaction complex **2** is calculated 3 and 5.5 kcal mol^{-1} more stable than reaction interaction complexes **1a** and **1b**, respectively, but 1.8 kcal mol^{-1} less stable than fully separated products. Therefore, a typical asymmetric double-well energy profile with a late transition state was obtained.

In addition to the spontaneous dissociation process $\mathbf{2} \rightarrow NH_2Cl + HCl$ (Fig. 1), the complex **2** can undergo a protonation, as well, in which the unstable $[NH_3Cl]^+Cl^-$ (**2′**) salt is formed (Scheme 2). The synthesis and characterization of the first stable $[NH_3Cl]^+M^-$ salts ($M = BF_4$, AsF_6, of SbF_6) have been reported recently.[70] It is shown that these simple inorganic cations with an N—Cl bond can be easily formed from monochloramine in the presence of a strong Lewis acid. Structure and reactivity of its protomer, $[NH_2ClH]^+$, have also been reported. It is found that the chlorine-protonated form is less stable by 41 kcal mol^{-1}.[71]

The symmetrical structure **2** (Cs point group) can be characterized as an ion-pair complex which is similar to the product of Menshutkin reaction,[72,73] but is also related to the S_N2 nucleophilic displacement reaction on neutral nitrogen[74] or at saturated carbon.[75–79] In the gas phase, due to the charge separation, the $[NH_3Cl]^+$ salt **2′** is significantly destabilized (by more than 15 kcal mol^{-1} at the B3LYP level) when compared to the hydrogen-bonded product **2**. These two product complexes, **2** and **2′**, are connected through the transition state structure $\mathbf{TS_{2-2'}}$ (Scheme 2). The transition state $\mathbf{TS_{2-2'}}$ is calculated only 0.6 kcal mol^{-1} less stable than **2′**, and is characterized by one imaginary frequency ($117i\,cm^{-1}$) which corresponds to the hydrogen shift from the nitrogen atom to the chlorine ion.

However, the structure **2′** is also controversial (at least in the case when the Cl^- is a counterion) as both MPWB1K and M05-2X methods cannot locate this structure as a real minimum, but converges to separated products NH_2Cl and HCl. It is due to the chlorine as a counterion, since we can easily locate such a type of salt when BF_4^- is used as a counterion (i.e., $[NH_3Cl]^+[BF_4]^-$, see Supplementary Information), which is much less nucleophilic than Cl^-. This is in agreement with experimental results presented above.[70]

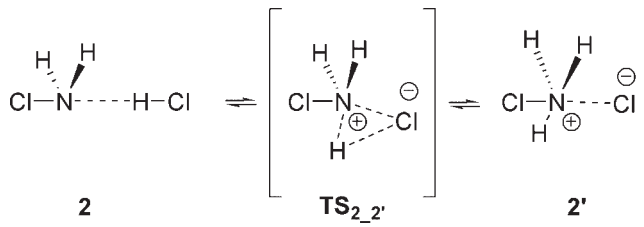

Scheme 2.

Along with the pathways A and B, the third possible pathway C has also been considered (Fig. 1). According to this pathway C, the rearrangement starts from **1a** which undergoes an uphill hydrogen shift, from the nitrogen to the chlorine atom, forming a high-energy intermediate **3**. The transition state structure **TSc** (Fig. 2) for this process is more than 15 kcal mol^{-1} higher in energy (at all levels employed) than transition state structures **TSa** and **TSb** which correspond to the pathway A and B, respectively (Table 1). The second hydrogen shift between two chlorine atoms converts the intermediate **3**, through the bridged transition state structure **TSc′**, to the more stable (for *ca.* 60 kcal mol^{-1}) intermediate **2**. It is interesting that both the intermediate structure **3** and transition structure **TSc′** do not exist on the potential energy surface calculated at B1B95 and MPWB1K levels. According to these functionals the linear complex **1a** is directly converted to **2** via the transition structure **TSc**. If the fraction of HF exchange (χ) in the functional is increased (e.g., M05-2X; $\chi = 56$) the mechanism of the pathway C shifts to the two steps consecutive process $\mathbf{1a} \rightarrow \mathbf{TSc} \rightarrow \mathbf{3} \rightarrow \mathbf{TSc'} \rightarrow \mathbf{2}$.

Therefore, three possible routes for the chlorination of NH_3 by Cl_2 in the gas phase were located on the corresponding PES. Pathways A and B are kinetically equally plausible since both proceed through barriers (**TSa** or **TSb**, respectively) that are similar in energy. However, the existence of the transition structure **TSa** is somewhat controversial (see above). The third pathway C involves the intermediate **3**, and two hydrogen-bridged transition states, **TSc** and **TSc′**, and all of them are very unstable structures, which makes this chlorination mechanism quite unlikely, at least in the case of ammonia.

In general, both geometries and relative energies of all structures involved in pathways A, B, or C are dependent on the density functional applied. These results suggest that it is mandatory to compare results obtained at different theoretical levels, since both geometries and energies are not only influenced but also a complete mechanistic picture could be significantly changed. We have noticed that by increasing the fraction of HF exchange in the functionals, the DFT results converge to that calculated at the MP2 level of theory. This suggests, in line with earlier findings,[65,66] that the M05-2X functional ($\chi = 56$) is the most reliable for an accurate description of the chlorination mechanism. Therefore, this functional was selected, along with the most popular B3LYP, for calculations of medium and substituent effects on the N-chlorination reaction.

MEDIUM EFFECTS

Contrary to the Menshutkin type of reaction, where the two neutral reactants result in separated ion product, and are therefore very sensitive to polarizability of the medium,[80–82] the reaction between ammonia and chlorine via **TSa** or **TSb** directly produces two neutral product molecules, i.e., NH_2Cl and HCl. It is shown that the calculated bulk solvent effect of dimethyl sulfoxide (DMSO, $\varepsilon = 46.7$) on the energetics of the Menshutkin reaction between ammonia and methyl chloride is significant.[47] The reaction activation free energy in DMSO decreases by more than 16 kcal mol^{-1} with respect to the gas phase (from 41.9 to

25.5 kcal mol^{-1}, respectively), and the corresponding transition state is shifted considerably to an earlier stage of the reaction (the transition state becomes more reactant-like). For comparison, we have performed the same solvent model calculations (SCIPCM geometry optimizations and numerical frequency calculations in DMSO) for the chlorination of NH_3 by Cl_2. As expected, the calculated reaction field effect is much less pronounced for this chlorination reaction. At B3LYP level the calculated activation free energy for the pathway A in DMSO is 42.5 kcal mol^{-1}, which is only 4.4 kcal mol^{-1} lower than the corresponding gas-phase value. As well, only small changes in geometry of **TSa** are calculated during optimization procedure in the presence of the model solvent, which confirms that the chlorination reaction of ammonia is not very susceptible to bulk solvation effects. For example, the bond distance between the two chlorine atoms in the transition structure **TSa** (Fig. 2) is shortened (2.600 Å) compared to the gas-phase structure (2.707 Å), while the distance between nitrogen and chlorine atoms is slightly elongated (2.418 Å *vs.* 2.337 Å, respectively). As expected, these structural changes on going from the gas phase to the solvent ($\varepsilon = 46.7$) are consistent with a slight shift of the transition state **TSa** to an earlier stage of the reaction.

Interestingly, in the solvent model the pathway B is calculated for 0.6 kcal mol^{-1} more favorable than the pathway A (Table 1), while the pathway C has, similar to the gas-phase calculations, very high-energy barrier. Similar to the gas-phase calculations, no transition structure with "eclipsed" conformation (**TS** can be located if meta hybrid functionals are employed for solvent model (SCIPCM) calculations. Only the "staggered" transition structure **TSb** is found at the corresponding PES. The calculated energy barrier for this pathway B is only slightly influenced when solvent model is taken into account. At the SCIPCM-M05-2X level the calculated energy barrier for the process **1b** → **TSb** → **2** is 51.6 kcal mol^{-1}, which is only 5.7 kcal mol^{-1} lower that the calculated barrier in the gas phase.

Whereas the use of the solvent's bulk dielectric constant is justified in many cases, this is not the case with hydrogen bonding solvents such as water. To consider specific solvent interactions with intermediates involved in the reaction between ammonia and chlorine, a discrete water molecule is included in the solvent modeling calculations. It is suggested that in order to correctly calculate solvent effects on the chlorination of NH_3 by HOCl in aqueous solution, it is necessary to take into account the presence of explicit water molecules.[13] Therefore, in addition to implicit solvation as calculated by the SCIPCM continuum model, we have performed calculations which include specific solvent–solute interactions. It is found that an additional water molecule significantly influences this reaction, in particular by stabilizing transition state structures **TSa$_w$** and **TSb$_w$** (Fig. 3). The structure **TSa$_w$**, which is related to the pathway A in the gas phase, adopts a six-membered ring geometry with approximately linear arrangements of six atoms involved in an intramolecular rearrangement process. At B3LYP and M05-2X levels, it is characterized by one imaginary frequency (291*i* cm^{-1}; M05-2X) which corresponds to the simultaneous transfer of the two hydrogen atoms (from N to O and from O to Cl, respectively) coupled with N—Cl bond forming and Cl—Cl bond breaking processes. The inclusion of water molecule in this structure facilitates the Cl transfer from the chlorine molecule to ammonia, yielding a substantial reduction of the free energy barrier. The calculated barriers for the chlorination of NH_3 in the gas phase are 46.9 kcal mol^{-1} (B3LYP; pathway and 57.3 (M05-2X; pathway B)), whereas the

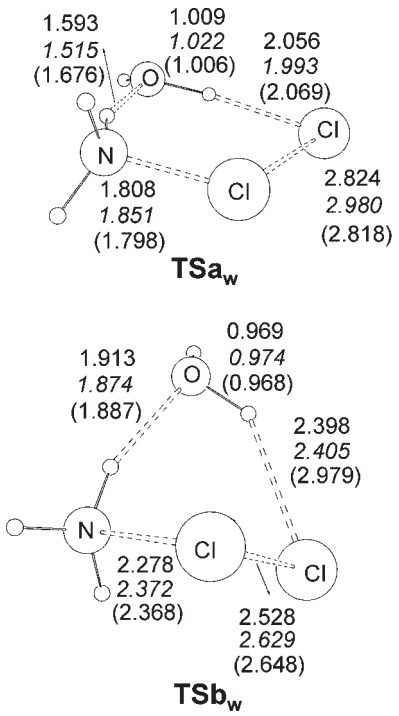

Figure 3. M05-2X/6–31 + G(d,p) optimized geometries of transition state structures TSaw and TSbw for the water-assisted chlorination of NH_3. Bond distances are in angstroms (B3LYP values in italics and MP2 values in parentheses)

corresponding barriers for water-assisted chlorination are reduced to 33.2 and 33.3 kcal mol^{-1}, respectively. The IRC procedure, performed by stepping forward and backward from the transition structure **TSa$_w$** along the imaginary mode, shows that this transition state leads to water-complexed reactant and product intermediates **1a$_{w1}$** and **2a$_{w1}$**, respectively (see below).

Similar to the **TSa$_w$**, the transition state structure **TSb$_w$**, which is related to the pathway B in the gas phase, also adopts a six-membered ring geometry (Fig. 3). The analogous transition state structure with a nonlinear arrangement was not considered in the earlier computational study[13] of the water-assisted chlorination of NH_3 by HOCl. However, due to the staggered conformation (B3LYP and M05-2X calculated Cl—Cl—N—H dihedral angle values are 172° and 167°, respectively) this structure cannot adopt a planar geometry, as required for an efficient water-assisted Cl transfer. Whereas the energy difference between transition state structures **TSa** and **TSb** is almost negligible, suggesting that pathways A and B in the gas phase are energetically similar, their water-complexed analogs **TSa$_w$** and **TSb$_w$**, respectively, differ for more than 14 kcal mol^{-1}. Since the **TSb$_w$** is significantly less stable than **TSa$_w$**, it appears that the pathway B could not be operative in the water environment. The similarity was found at the MP2 level where the **TSb$_w$** is calculated almost 17 kcal mol^{-1} less stable than the **TSa$_w$** (Table 2). Therefore, in the gas phase the two structures **TSa** and **TSb** are to be considered as rate-determining transition states, although the former is somewhat controversial (see above), whereas in the water solvent only the reaction route involving the transition state structure **TSa$_w$** is energetically plausible.

Interactions of water molecule with reactant and product intermediates of pathway A were also considered. Several water

Table 2. Relative[a] free energy (ΔG)[b] differences (in kcal mol^{-1}) for intermediates, transition state structures involved in the water-assisted chlorination of NH_3, with BSSE corrected values (ΔG^{CP}) for selected structures[c]

	B3LYP	M05-2X	MP2
Structure	ΔG (ΔG^{CP})	ΔG	ΔG
$NH_3 + Cl_2 + H_2O$	2.1	2.6	5.0
$1a_{w1}$	5.0 (6.4)	6.5	10.5
$1a_{w2}$	7.0 (7.9)	—	—
TSa_w	35.3 (37.6)	35.9	43.0
TSb_w	49.7 (51.2)	58.3	59.9
$2a_{w1}$	3.3 (5.3)	1.1	2.2
$2a_{w2}$	3.5 (5.5)	2.3	2.1
$NH_2Cl + HCl + H_2O$	0 (0)	0	0

[a] Relative energies with respect to separated products NH_2Cl, HCl, and H_2O.
[b] At 298.15 K.
[c] Basis set 6–31 + G(d,p) used throughout.

complexes of **1a** were optimized, but all converged to the two different complexes $\mathbf{1a_{w1}}$ and $\mathbf{1a_{w2}}$ (Scheme 3). At the M05-2X and MP2 levels only the cyclic complex $\mathbf{1a_{w1}}$ was located as a minimum. At the B3LYP level the complex $\mathbf{1a_{w1}}$ is calculated for 1 kcal mol^{-1} more stable than $\mathbf{1a_{w2}}$. In these complexes six atoms interacting in the transition structure $\mathbf{TSa_w}$ are already positioned in linear arrangement, but only the water complex $\mathbf{1a_{w1}}$ is directly connected to the $\mathbf{TSa_w}$, as calculated by the IRC procedure. The interaction distance between ammonia and chlorine moieties in water complexes $\mathbf{1a_{w1}}$ and $\mathbf{1a_{w2}}$ is shortened by 0.1 Å when compared to the corresponding N···Cl distance in **1a**. Contrary to the case of the transition structure $\mathbf{TSa_w}$ which is stabilized by one discrete water molecule insertion, the interaction of **1a** with water makes it, surprisingly, less stable than the corresponding structure of **1a** in the gas phase. This is probably due to the entropic contribution, which disfavors the formation of cyclic structures.

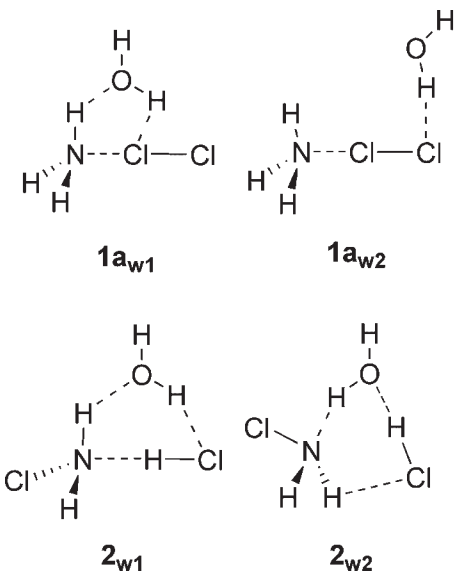

Scheme 3.

As well, several water complexes of the hydrogen-bonded product **2a** were attempted, but all starting geometries converged to the two stable isomers $\mathbf{2a_{w1}}$ and $\mathbf{2a_{w2}}$ (both at the B3LYP and MP2 levels). Both of these complexes (Scheme 3) are characterized by a six-membered ring geometry in which water molecule acts as both proton donor and acceptor. They are slightly destabilized with respect to the gas-phase product intermediate **2a**, mostly due to the entropic contribution, as discussed above. Interaction of water with intermediates **1b** and **2b** was not considered, since it is found that the pathway B is not an operative mechanism in water.

According to these computational results, one can conclude that the inclusion of a discrete water molecule results in measurable differences in geometry in both transition state structures and intermediates, and influences not only the energetics of the chlorination reaction but also the overall mechanism, which is significantly changed. While this water-assisted mechanism could be related to treatment procedures such as chlorination of potable water or wastewaters, pathways A and B should be considered, however, in cases where no water assistance is possible. As already mentioned earlier, there is a number of hydrophobic media in which no water participation is to be expected. Such chlorination reactions occur in the gas phase, in organic solvents, or in the active site of enzymes, to name but a few chlorinations that are relevant to both environmental chemistry and biochemistry. In these cases the amine-containing compounds undergo the direct reaction with Cl_2 (not catalyzed by water).

To estimate the size of the basis set superposition error (BSSE) on the interaction energies of intermediate complexes and transition states involved in both chlorination reactions (the pathway A in the gas phase and the water-catalyzed mechanism), the popular counterpoise (CP) method was employed.[48] Since the BSSE introduces an artificial attractive force between the fragments (chlorine, ammonia, or water, in our case), CP corrections usually lead to less stable complexes with larger optimized intermolecular distances as compared to CP-uncorrected optimized systems.[83–85] Thus, we have used the CP to correct both the optimized geometries and the interaction energies, i.e., the CP corrections were considered over the whole PES for each particular chlorination reaction.

As expected, it is found that the N—Cl interaction distances in both **1a** (2.438 Å) and its water-complex $\mathbf{1a_{w1}}$ (2.344 Å), are calculated somewhat longer (2.462 Å and 2.369, respectively) when the CP correction is introduced. The similarity was found for **TSa** and its water-complex analogue $\mathbf{TSa_w}$. As well, the distance of the hydrogen bond N···H(Cl) in the interaction product **2a** (1.823 Å) and its water-complex $\mathbf{2a_{w1}}$ (1.635 Å) where calculated slightly longer after BSSE correction (1.882 and 1.694 Å, respectively).

Along with these negligible geometry changes upon CP-optimizations, some minor changes in interaction energies were also calculated when CP correction is performed (Table 2). The calculated free energy barriers for the pathway A chlorination and for the water-assisted chlorination are higher for 0.7 kcal mol^{-1} and 2.3 kcal mol^{-1}, respectively, when the CP correction is included. Therefore, decrease of the energy barrier calculated for the water-catalyzed mechanism, when compared to the gas-phase pathway A, is mostly due to the water

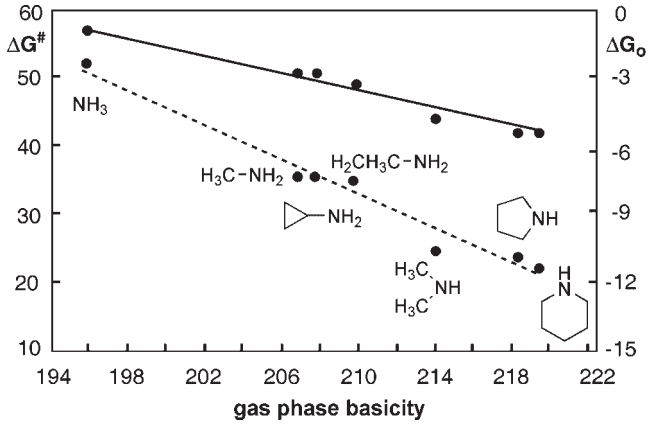

Figure 4. Dependence of the M05-2X calculated reaction energy (ΔG_o; dashed line) and calculated free energy barrier ($\Delta G^{\#}$; solid line) of the chlorination of amines by Cl_2 on the experimental gas-phase basicity (in kcal mol^{-1}) of different amines

participation alone, and only minor contribution comes from the BSSE error.

SUBSTITUENT EFFECTS

Since the free electron pair on the nitrogen is directly involved in the formation of **1a**, the most stable encounter complex, the chlorination reaction of NH_3 by Cl_2 is similar to an S_N2 reaction (type II S_N2 reaction analogous to the Menshutkin reaction),[49] or nucleophilic displacement, and the rate of reaction should vary as the base strength of the nitrogen compound. Indeed, we have calculated that free energy barriers for the chlorination of aliphatic amines by Cl_2 decrease with the increase in the gas-phase basicity (GB) of the amines (Fig. 4). Only the "staggered" transition state structures were considered (analogous to **TSb**) at the M05-2x level, since the transition structures with an "eclipsed" conformation (as measured by the Cl—Cl—N—H dihedral angle) were calculated less stable and all were characterized as the second-order stationary points. In the case of the cyclopropylamine the transition state structure with an eclipsed conformation was located, but was calculated *ca.* 1 kcal mol^{-1} less stable than the staggered conformer. For example, the calculated $\Delta G^{\#}$ for the chlorination of $(CH_3)_2NH$ (GB = 214.3) and piperidine (GB = 220.0) are 42.6 kcal mol^{-1} and 42.4 kcal mol^{-1}, respectively, both values being lower than the corresponding free energy barriers for the chlorination of $(CH_2)_2CHNH_2$ (GB = 207.9; $\Delta G^{\#}$ = 50.1 kcal mol^{-1}) and CH_3NH_2 (GB = 206.6; $\Delta G^{\#}$ = 48.5 kcal mol^{-1}).[86] The highest energy barrier has been calculated for the chlorination of NH_3 (57.3 kcal mol^{-1}; Pathway B), which is the least basic (GB = 195.7). This strongly indicates a nucleophilic attack by the N atom of the amine on the Cl atom in the chlorine molecule as the rate-determining step in the reaction mechanism. It is in agreement with experimental data available for the chlorination of amines by HOCl where the similar reaction mechanism is expected.[87,88] A linear regression of the calculated activation energies with the experimental gas-phase basicities (Fig. 4) gives a correlation coefficient $r = 0.96$ (the slope is −0.67, and the value of the intercept is 187.58). This linearity indicates that nucleophilic reactivities of different amines toward the Cl_2, for which experimental values could not be accessible, could be reliably predicted by using modern DFT methods.

The thermodynamics of the chlorination reaction of amines is dependent on the subsequent introduction of N-substituents, as well. The equilibrium constants for reactions $R_1R_2NH + Cl_2 \leftrightarrows R_1R_2N - Cl + HCl$ should become larger as the substituted amines become more basic. Indeed, it is found that the reaction free energy (ΔG_o) for chlorination of piperidine ($\Delta G_o = -11.6$ kcal mol^{-1}) is larger than the corresponding calculated values for chlorination of CH_3NH_2 ($\Delta G_o = -7.4$ kcal mol^{-1}) or NH_3 ($\Delta G_o = -2.6$ kcal mol^{-1}). The values of the calculated reaction free energies plotted against the experimental gas-phase basicities exhibit excellent linearity ($r = 0.97$, the value of the slope is −0.37, and the intercept is 69.12). These results suggest that the chlorination of amines by Cl_2 is both kinetically and thermodynamically more favorable process when more basic amine is employed. Thus, it is confirmed that the experimental findings could be successfully reproduced by an appropriate DFT method, at least for certain subgroups of amine substrates, which demonstrates again the predictive value of such a quantum chemical approach.

With the increase in the basicity of the amine, the transition state for the corresponding chlorination is shifted to an earlier stage of reaction, i.e., the transition state structure becomes more reactant-like. On going from NH_3 to CH_3NH_2 and $(CH_2)_5NH$ (piperidine), the interaction distance between N and Cl atoms is successively elongated (2.215, 2.249, and 2.312 Å, respectively), while the Cl—Cl bond is shortened (2.593, 2.554, and 2.522 Å, respectively). These results illustrate a fine correlation between a degree of the Cl—Cl bond dissociation in the transition state and the value of the free energy barrier (see above). The higher barrier is associated with a larger deformation (stretching) of the Cl—Cl bond, i.e., with the more extensive bond cleavage of the leaving group in the transition state. For example, the M05-2X calculated imaginary frequencies (N—Cl stretch vibrational modes) for $NH_3\cdots Cl_2$, $CH_3NH_2\cdots Cl_2$, and $(CH_2)_5NH\cdots Cl_2$ complexes are 455*i*, 436*i*, and 373*i* cm^{-1}, respectively. These findings are in agreement with earlier quantum-chemical calculations on S_N2 reactions at neutral nitrogen[74] and carbon analogues.[89,90]

CONCLUSION

A detailed mechanism for the reaction between ammonia and chlorine in the gas phase was investigated. The number of available density functionals were used for calculations including the generalized gradient approximation or GGA, the meta GGA, the hybrid GGA, and finally the hybrid meta GGA. As expected, the performance of HM-GGA and H-GGA methods is better than local functionals.[91] In particular, the M05-2X functional gives the best performance for the calculation of noncovalent interactions found in charge-transfer (e.g., **1a**, **1a′**, or **2c**) and hydrogen-bonding complexes (e.g., **1b**, **1b′**, or **2a**), as suggested earlier.[65,66]

Several new intermediates and transition state structures were located and two alternative reaction pathways, along the pathway A, were proposed (pathways B and C). The solvent modeling calculations (in DMSO) and specific interactions of intermediates and transition states with water molecules were considered. The calculated reaction field effects on both

structural changes and relative energies of intermediates are negligible. However, it is found that transition state structures **TSa_w** and **TSb_w** are preferentially stabilized over the reactants when explicit water molecule is included. It is also found that nucleophilic reactivity of aliphatic amines toward the Cl_2 correlates with basicity of the corresponding amines.

In addition, the DFT results were compared to those obtained at the MP2 level of theory. Density functionals with high fraction of HF exchange produced results that were found to be the most similar to those obtained with the second-order perturbation theory. This comparative study suggests that different theoretical levels should be taken into account in determining the detailed mechanism of the chlorination reactions. In general, we have found that the combination of M05-2X and MP2 theoretical levels is essential for further studies of chlorination mechanism of various amine-containing compounds relevant to both environmental chemistry and biochemistry.

Acknowledgements

We thank the Computing Center SRCE of the University of Zagreb for allocating computer time on the Isabella cluster.

REFERENCES

[1] M. Bedner, W. A. MacCrehan, *Environ. Sci. Technol.* **2006**, *40*, 516–522.
[2] S. K. Khetan, T. J. Collins, *Chem. Rev.* **2007**, *107*, 2319–2364.
[3] J. Li, E. R. Blatchley, III *Environ. Sci. Technol.* **2007**, *41*, 6732–6739.
[4] E. M. Fiss, K. L. Rule, P. J. Vikesland, *Environ. Sci. Technol.* **2007**, *41*, 2387–2394.
[5] S. H. Joo, W. A. Mitch, *Environ. Sci. Technol.* **2007**, *41*, 1288–1296.
[6] Y. W. Yap, M. Whiteman, N. S. Cheung, *Cell. Signal.* **2007**, *19*, 219–228.
[7] S. Pennathur, J. W. Heinecke, *Antioxid. Redox Signal.* **2007**, *9*, 955–969.
[8] B. H. Shao, M. N. Oda, J. F. Oram, J. W. Heinecke, *Curr. Opin. Cardiol.* **2006**, *21*, 322–328.
[9] Y. Kawai, H. Kiyokawa, Y. Kimura, Y. Kato, K. Tsuchiya, J. Terao, *Biochemistry* **2006**, *45*, 14201–14211.
[10] C. L. Hawkins, D. I. Pattison, M. J. Davies, *Amino Acids* **2003**, *25*, 259–274.
[11] I. Weil, J. C. Morris, *J. Am. Chem. Soc.* **1949**, *71*, 1664–1671.
[12] L. Abia, X. L. Armesto, M. L. Canle, M. V. Garcia, J. A. Santaballa, *Tetrahedron* **1998**, *54*, 521–530.
[13] J. Andrés, M. L. Canle, M. V. García, L. F. Rodríguez Vázquez, J. A. Santaballa, *Chem. Phys. Lett.* **2001**, *342*, 405–410.
[14] S. L. Hazen, F. F. Hsu, D. M. Mueller, J. R. Crowley, J. W. Heinecke, *J. Clin. Invest.* **1996**, *98*, 1283–1289.
[15] S. L. Hazen, F. F. Hsu, K. Duffin, J. W. Heinecke, *J. Biol. Chem.* **1996**, *271*, 23080–23088.
[16] J. P. Henderson, J. Byun, J. W. Heinecke, *J. Biol. Chem.* **1999**, *274*, 33440–33448.
[17] E. A. Voudrias, M. Reinhard, *Environ. Sci. Technol.* **1988**, *22*, 1049–1056.
[18] D. W. Margerum, E. T. Gray, R. P. Huffman, in *Organometals, Organometalloids, Occurrence, Fate in the Environment*, (Eds.: F. E. Brinckman, J. M. Belloma) American Chemical Society, Washington, DC, **1979**, pp. 278–291.
[19] E. Grimley, G. Gordon, *J. Phys. Chem.* **1973**, *77*, 973–978.
[20] F. E. Scully, Jr., W. N. White, *Environ. Sci. Technol.* **1991**, *25*, 820–828.
[21] H. H. Sisler, F. T. Neth, R. S. Drago, D. Yaney, *J. Am. Chem. Soc.* **1954**, *76*, 3906–3909.
[22] J. M. Cheplen, C. Barrow, E. L. White, *Anal. Chem.* **1984**, *56*, 1194–1196.
[23] C. S. Barrow, D. E. Dodd, *Toxicol. Appl. Pharmacol.* **1979**, *49*, 89–95.
[24] M. Y. Fukayama, T. Tan, W. B. Wheeler, C.-I. Wei, *Environ. Health Persp.* **1986**, *69*, 267–274, and references therein.
[25] M. J. Frisch, G. W. Trucks, H. B. Schlegel, G. E. Scuseria, M. A. Robb, J. R. Cheeseman, J. A. Montgomery, Jr., T. Vreven, K. N. Kudin, J. C. Burant, J. M. Millam, S. S. Iyengar, J. Tomasi, V. Barone, B. Mennucci, M. Cossi, G. Scalmani, N. Rega, G. A. Petersson, H. Nakatsuji, M. Hada, M. Ehara, K. Toyota, R. Fukuda, J. Hasegawa, M. Ishida, T. Nakajima, Y. Honda, O. Kitao, H. Nakai, M. Klene, X. Li, J. E. Knox, H. P. Hratchian, J. B. Cross, C. Adamo, J. Jaramillo, R. Gomperts, R. E. Stratmann, O. Yazyev, A. J. Austin, R. Cammi, C. Pomelli, J. W. Ochterski, P. Y. Ayala, K. Morokuma, G. A. Voth, P. Salvador, J. J. Dannenberg, V. G. Zakrzewski, S. Dapprich, A. D. Daniels, M. C. Strain, O. Farkas, D. K. Malick, A. D. Rabuck, K. Raghavachari, J. B. Foresman, J. V. Ortiz, Q. Cui, A. G. Baboul, S. Clifford, J. Cioslowski, B. B. Stefanov, G. Liu, A. Liashenko, P. Piskorz, I. Komaromi, R. L. Martin, D. J. Fox, T. Keith, M. A. Al-Laham, C. Y. Peng, A. Nanayakkara, M. Challacombe, P. M. W. Gill, B. Johnson, W. Chen, M. W. Wong, C. Gonzalez, J. A. Pople, *Gaussian 03, Revision E.01*, *Gaussian, Inc., Wallingford, CT* (**2004**).
[26] C. Lee, W. Yang, R. G. Parr, *Phys. Rev. B* **1988**, *37*, 785–789.
[27] Y. Zhao, N. E. Schultz, D. G. Truhlar, *J. Chem. Phys.* **2005**, *123*, 161103.
[28] J. Tao, J. P. Perdew, V. N. Staroverov, G. E. Scuseria, *Phys. Rev. Lett.* **2003**, *91*, 146401.
[29] C. Lee, W. Yang, R. G. Parr, *Phys. Rev. B* **1988**, *37*, 785.
[30] A. D. Becke, *J. Chem. Phys.* **1993**, *98*, 5648.
[31] P. J. Stevens, F. J. Devlin, C. F. Chablowski, M. J. Frisch, *J. Chem. Phys.* **1994**, *98*, 11623.
[32] For general performance of B3LYP methods for a large set of organic molecules, see: J. Tirado-Rives, W. L. Jorgensen, *J. Chem. Theory Comput.* **2008**, *4*, 297–306.
[33] A. D. Becke, *J. Chem. Phys.* **1996**, *104*, 1040–1046.
[34] A. D. Becke, *Phys. Rev. A* **1988**, *38*, 3098–3100.
[35] C. Adamo, V. Barone, *J. Chem. Phys.* **1998**, *108*, 664–675.
[36] Y. Zhao, D. G. Truhlar, *J. Phys. Chem. A* **2004**, *10*, 6908–6918.
[37] Y. Zhao, N. E. Schultz, D. G. Truhlar, *J. Chem. Theory Comput.* **2006**, *2*, 364–382.
[38] Y. Zhao, D. G. Truhlar, *Theor. Chem. Acc.* **2008**, *120*, 215–241.
[39] C. Moller, M. S. Plesset, *Phys. Rev.* **1934**, *46*, 618–622.
[40] M. J. Frisch, M. Head-Gordon, J. A. Pople, *Chem. Phys. Lett.* **1990**, *166*, 275–280.
[41] C. Gonzales, H. B. Schlegel, *J. Phys. Chem.* **1990**, *94*, 5523–5527.
[42] J. B. Foresman, T. A. Keith, K. B. Wiberg, J. Snoonian, M. J. Frisch, *J. Phys. Chem.* **1996**, *100*, 16098–16104.
[43] K. B. Wiberg, S. Clifford, W. L. Jorgensen, M. J. Frisch, *J. Phys. Chem. A* **2000**, *104*, 7625–7628.
[44] A. Bagno, G. Modena, *Eur. J. Org. Chem.* **1999**, 2893–2897.
[45] P. K. Chattaraj, P. Perez, J. Zevallos, A. Toro-Labbe, *J. Phys. Chem. A* **2001**, *105*, 4272–4283.
[46] H. Castejon, K. B. Wiberg, S. Sklenak, W. Hinz, *J. Am. Chem. Soc.* **2001**, *123*, 6092–6097.
[47] H. Castejon, K. B. Wiberg, *J. Am. Chem. Soc.* **1999**, *121*, 2139–2146.
[48] S. F. Boys, F. Bernardi, *Mol. Phys.* **1970**, *10*, 553–566.
[49] Eds.: M. B. Smith, J. March *March's Advanced Organic Chemistry: Reactions, Mechanisms, Structure* (6th edn). John Wiley & Sons, Inc., Hoboken, NJ, **2007**, pp. 430, 555, and references therein.
[50] A. C. Legon, D. G. Lister, J. C. Thorn, *J. Chem. Soc., Chem. Commun.* **1994**, 757–758.
[51] A. C. Legon, D. G. Lister, J. C. Thorn, *J. Chem. Soc. Faraday Trans.* **1994**, *90*, 3205–3212.
[52] R. R. Lucchese, H. F. Schaefer, III *J. Am. Chem. Soc.* **1975**, *97*, 7205–7210.
[53] I. Røeggen, T. Dahl, *J. Am. Chem. Soc.* **1992**, *114*, 511–516.
[54] A. E. Reed, F. Weinhold, L. A. Curtiss, D. J. Pochatko, *J. Chem. Phys.* **1986**, *84*, 5687–5705.
[55] H. Umeyama, K. Morokuma, S. Yamabe, *J. Am. Chem. Soc.* **1977**, *99*, 330–335.
[56] E. Ruiz, D. R. Salahub, A. Vela, *J. Phys. Chem.* **1996**, *100*, 12256–12276.
[57] H. I. Bloemink, K. Hinds, A. C. Legon, J. C. Thorn, *Chem. Phys. Lett.* **1994**, *223*, 162–166.
[58] G. Ribbegard, *Chem. Phys. Lett.* **1974**, *25*, 333.
[59] J. A. Parr, G. Li, I. Fedorov, A. J. McCaffery, H. Reisler, *J. Phys. Chem. A* **2007**, *111*, 7589–7598.
[60] J. A. Altmann, M. G. Govender, T. A. Ford, *Mol. Phys.* **2005**, *103*, 949–961.
[61] T. A. Beu, U. J. Buck, *Chem. Phys.* **2001**, *114*, 7853–7858.
[62] D. M. Rayner, L. Lian, R. Fournier, S. A. Mitchell, P. A. Hackett, *Phys. Rev. Lett.* **1995**, *74*, 2070–2073.
[63] A. van der Avoird, E. T. H. Olthof, P. E. S. Wormer, *Faraday Discuss.* **1994**, *97*, 43–55.
[64] J. Wu, J. Zhang, Z. Wang, W. Cao, *J. Chem. Theory Comput.* **2007**, *3*, 95–102.

[65] E. Ruiz, D. R. Salahub, A. Vela, *J. Am. Chem. Soc.* **1995**, *117*, 1141–1142.
[66] Y. Zhao, D. G. Truhlar, *J. Chem. Theory Comput.* **2005**, *1*, 415–432.
[67] B. Bogdanov, T. B. McMahon, *J. Phys. Chem. A* **2006**, *110*, 1350–1363.
[68] M. N. Glukhotsev, A. Pross, H. B. Schlegel, R. B. Bach, L. Radom, *J. Am. Chem. Soc.* **1996**, *118*, 11258–11264.
[69] H. Bürger, *Angew. Chem. Int. Ed. Engl.* **1997**, *36*, 718–721.
[70] S. Schneider, R. Haiges, T. Schroer, J. Boatz, K. O. Christe, *Angew. Chem. Int. Ed.* **2004**, *43*, 5213–5217.
[71] A. Ricci, M. Rosi, *J. Phys. Chem. A* **1998**, *102*, 10189–10194.
[72] A. N. Jay, K. A. Daniel, E. V. Patterson, *J. Chem. Theory Comput.* **2007**, *3*, 336–343.
[73] E. Owczarek, W. Kwiatkowski, M. Lemieszewski, A. Mazur, M. Rostkowski, P. Paneth, *J. Org. Chem.* **2003**, *68*, 8232–8235.
[74] M. Bühl, H. F. Schaefer, *J. Am. Chem. Soc.* **1993**, *115*, 9143–9147.
[75] A. Ebrahimi, M. Habibi, A. Amirmijani, *Theochem-J. Mol. Struct.* **2007**, *809*, 115–124.
[76] S.-Y. Yang, P. F. Lessard, I. Hristov, T. Ziegler, *J. Phys. Chem. A* **2004**, *108*, 9461–9468.
[77] I. Lee, C. K. Kim, C. K. Sohn, H. G. Li, H. W. Lee, *J. Phys. Chem. A* **2002**, *106*, 1081–1087.
[78] S. Parthiban, G. de liveira, J. M. L. Martin, *J. Phys. Chem. A* **2001**, *105*, 895–904.
[79] M. N. Glukhovtsev, A. Pross, H. B. Schlegel, R. D. Bach, L. Radom, *J. Am. Chem. Soc.* **1996**, *118*, 11258–11264.
[80] For solvents effects, see: M. Higashi, S. Hayashi, S. Kato, *J. Chem. Phys.* **2007**, *126*, 144503–144513.
[81] A. Melo, A. J. I. Alfaia, J. C. R. Reis, A. R. T. Calado, *J. Phys. Chem. B* **2006**, *110*, 1877–1888.
[82] S. P. Webb, M. S. Gordon, *J. Phys. Chem. A* **1999**, *103*, 1265–1273.
[83] S. Simon, M. Duran, J. J. Dannenberg, *J. Chem. Phys.* **1996**, *105*, 11024–11031.
[84] P. Salvador, M. Duran, J. J. Dannenberg, *J. Phys. Chem A* **2002**, *106*, 6883–6889.
[85] N. Kobko, J. J. Dannenberg, *J. Phys. Chem A* **2001**, *105*, 1944–1950.
[86] *Experimental GB values from: NIST Chemistry WebBook, NIST Standard Reference Database Number 69, Linstron*, P. J; Mallard, W. G., Eds.: National Institute of Standards, Technology, Gaithersburg, MD, http://webbook.nist.gov, June (**2005**).
[87] X. L. Armesto, M. L. Canle, M. V. García, J. A. Santaballa, *Chem. Soc. Rev.* **1998**, *27*, 453–460.
[88] J. M. Antelo, F. Arce, M. Parajo, A. I. Pousa, J. C. Pérez-Moure, *Int. J. Chem. Kinet.* **1995**, *27*, 1021–1031.
[89] S. S. Shaik, H. B. Schlegel, S. Wolfe, *J. Chem. Soc., Chem. Commun.* **1988**, 1322–1324.
[90] S. S. Shaik, A. Ioffe, A. C. Reddy, A. Pross, *J. Am. Chem. Soc.* **1994**, *116*, 262–273.
[91] S. F. Sousa, P. A. Fernandes, M. J. Ramos, *J. Phys. Chem A* **2007**, *111*, 10439–10452, and references therein.